Optical probes of π-conjugated polymer blends with strong acceptor molecules

J. Holt,[1] S. Singh,[1] T. Drori,[1] Ye Zhang,[2] and Z. V. Vardeny[1,*]
[1]*Department of Physics, University of Utah, Salt Lake City, Utah 84112, USA*
[2]*Department of Materials Science & Engineering, University of Utah, Salt Lake City, Utah 84112, USA*
(Received 8 February 2009; revised manuscript received 4 May 2009; published 28 May 2009; corrected 30 June 2009)

We used a variety of optical probes to study the primary and long-lived photoexcitations in blends of polyphenylene-vinylene derivative poly(2-methoxy-5(2′-ethyl)hexoxy-phenylenevinylene) (MEH-PPV) with various concentrations of a *strong* electron-acceptor molecule 2,4,7-trinitro-9-fluorenone (TNF) for photovoltaic applications. The optical probes include fs transient photomodulation in a broad spectral range from 0.25 to 2.5 eV and a variety of cw spectroscopies such as steady-state photomodulation and its excitation spectrum, photoluminescence, and electroabsorption. With excitation above the polymer optical gap we found that the fs transient midinfrared-photoinduced absorption band and cw photoluminescence, which are both due to photogenerated excitons, are dramatically quenched in MEH/TNF blends with increasing TNF concentration. In addition significant charge-transfer (CT) species are also instantaneously photogenerated but they undergo fast geminate recombination within ~10 ps; this explains a major inefficiency of this blend for photovoltaic applications. Indeed, *I-V* measurement of a photovoltaic cell made from (1:1) MEH-PPV/TNF blend under illumination yields photocurrent density in the $\mu A/cm^2$ range, three orders smaller than a device made from MEH-PPV/C_{60} blend. Nevertheless the few photogenerated CT species that escape geminate recombination are subsequently captured in traps forming long-lived polarons. When using "below-gap" excitation in the near-infrared spectral range we found that short-lived CT species and long-lived polarons are also photogenerated with high quantum efficiency. This shows that a CT complex state is formed below the polymer optical gap in these blends, as verified by electroabsorption spectroscopy but has low dissociation efficiency; this is in contrast to polymer blends with fullerene molecules, where apparently the CT complex state below the gap has much higher dissociation efficiency.

DOI: 10.1103/PhysRevB.79.195210 PACS number(s): 78.55.Kz, 78.40.Fy, 78.40.Me, 78.47.−p

I. INTRODUCTION

Current development of organic solar cells based on bulk heterojunctions of donor-acceptor blends having up to ~6% power conversion efficiency, η requires understanding and control of photoinduced charge-transfer (CT) states and photoexcitation dynamics of excited donor-acceptor pairs. It has been shown that in the π-conjugated polymers both neutral (exciton) and charged (polaron) photoexcitations can be instantaneously generated[1] but quickly recombine unless the photogenerated charges are separated; this is accomplished in bulk-heterojunction architecture based on polymers by incorporating an electron-acceptor network. One current deficiency in organic solar cells however, is negligible absorption in the near-infrared (NIR) spectral range of the solar spectrum, which lies within the optical gap of most conventional organic blend systems. Several techniques have been developed to increase the near-infrared absorption including using lower-bandgap polymers,[2] multiactive layer devices,[3,4] and more recently, charge-transfer complexes.[5–12] However, devices made from low-bandgap polymers also yield low open-circuit voltage (V_{OC}), unless new acceptors are engineered. Multijunction solar cells that capture most of the solar spectrum are also used in the semiconductor industry to boost η but the devices become complex and expensive to manufacture. Multijunction devices also reduce short-circuit current, I_{SC} since they are wired in series; reducing V_{OC} or I_{SC}, in turn lower η. Thus none of the traditional techniques for increasing η in organic solar cells is ideal, which is impelling a search for more novel solutions. A viable candidate may be a polymer/acceptor blend with a molecular acceptor having *larger* electron affinity than the traditional fullerene molecules. Below-gap optical excitation of such organic donor/acceptor blends reveals subtle features attributed to charge-transfer complexes (CTC), which have recently attracted much attention by their property of extending optical absorption into the NIR spectral range. One proposal is to use 2,4,7-trinitro-9-fluorenone (TNF) [molecular structure given in Fig. 1(a) inset] as the strong acceptor.

When the π-conjugated poly(2-methoxy-5(2′-ethyl)hexoxy-phenylenevinylene) [MEH-PPV; molecular structure given in Fig. 1(b) inset] as electron donor and TNF are blended, new nonadditive optical transitions are observed.[5,6] Bakulin *et al.* reported that the absorption spectrum of such blends extends into the near-infrared spectral range [see Fig. 1(a)], along with a nonadditive photoluminescence (PL) band; new and shifted infrared-active vibrational bands and Raman-scattering spectra; and a new photoinduced absorption (PA) band. The polymer PL is strongly quenched, similar as in other polymer/fullerene blend systems.[13] In addition, TNF has a relatively high electron affinity[14] with a lowest unoccupied molecular-orbital (LUMO) energy difference from that of MEH-PPV *larger* than that of C_{60}; this should prevent electron back transfer after charge separation.[15] Such a body of evidence would nominate TNF as an exceptional candidate for bulk-heterojunction photovoltaic applications. In reality though, actual photocurrent in TNF devices was found to be[16] orders of magnitude lower than that in more conventional polymer/C_{60} blend devices. Yet TNF remains a model prototype for studying the influence of CTC states in organic

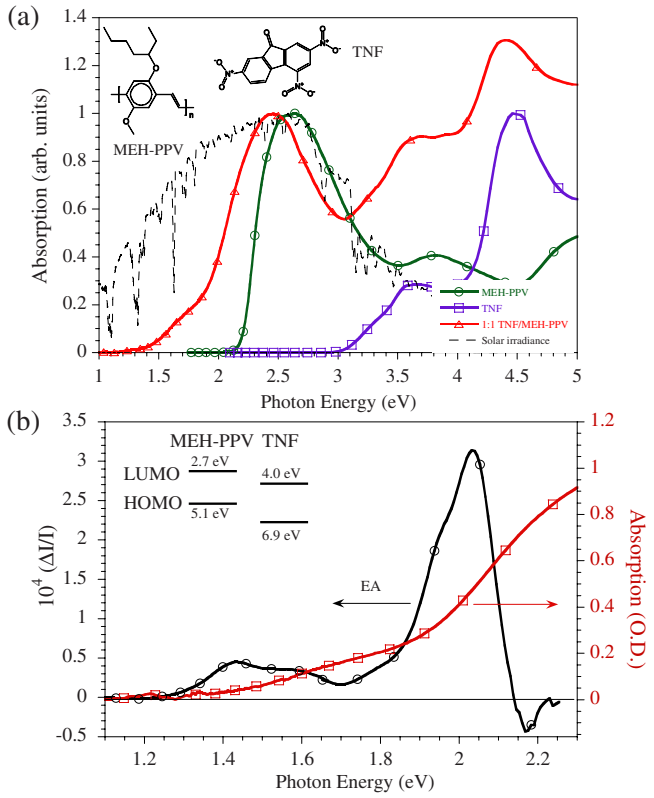

FIG. 1. (Color online) (a) Absorption spectra in a neat MEH-PPV film (green circles), TNF (violet squares), and 1:1 molar ratio MEH-PPV:TNF (red triangles). The solar irradiance spectrum (AM1.5; dashed line) is also shown for comparison. Inset shows the chemical structure of the polymer and TNF molecules. (b) Electroabsorption spectrum in a blend film (black circles) compared with the absorption spectrum (red squares). Inset depicts respective HOMO and LUMO energy levels of MEH-PPV (Ref. 36) and TNF (Ref. 37).

photovoltaics. Recently a series of significant followup works on polymer/TNF blends has been performed,[5–7] including the ultrafast dynamics measurements of an MEH-PPV doped with a low concentration of TNF molecules.[17]

In this paper we present additional support for the below-gap CTC formed in MEH-PPV/TNF blends with high TNF concentration, using several optical probes that include both ultrafast and cw spectroscopy techniques. We used ultrafast pump-probe transient photomodulation (PM) spectroscopy, which is excited at both below and above the polymer optical gap, and probed in an exceptionally broad spectral range from 0.2 to 2.0 eV photon energy having ~150 fs time resolution; whereas the cw techniques include absorption, electroabsorption, and steady-state PM and its action spectrum. Our optical investigation is complemented by fabricating and characterizing solar cell devices based on MEH-PPV/TNF blends. We verify the existence of below-gap CTC state using electroabsorption and action spectrum of the cw PA bands. By exciting *directly* into the CTC state we reveal well-resolved CTC PA bands that instantaneously form in the midinfrared (MIR) and near-infrared spectral range. However we found that the CT states decay very quickly to the ground state, within ~10 ps, which we interpret as due to geminate recombination. This ultrafast CT dynamics explains a significant underlying mechanism for the low efficiency of solar cells made from MEH-PPV/TNF blends, which show very low photocurrent. We compare our results to those in MEH-PPV/C_{60} blends and conclude that the photogenerated CT dissociation efficiency is significantly lower in MEH-PPV/TNF blends, probably because of the higher-TNF electron affinity.

II. EXPERIMENTAL

For the transient PM spectroscopy in the midinfrared spectral range we used the fs two-color pump-probe correlation technique with a low power (energy/pulse ~0.1 nJ), high-repetition rate (~80 MHz) laser system based on Ti:sapphire (Tsunami, Spectra Physics) and an optical parametric oscillator (OPO; Opal, Spectra Physics) having a probe spectral range from 0.24 to 1.1 eV using the signal, idler, and their nonlinear optical mixing. For the near-infrared/visible spectral range we used a high power (energy/pulse ~10 μJ), low-repetition rate (~1 kHz) laser with probe photon energy from 1.2 to 2.0 eV based on supercontinuum generation. The transient PM signal that was measured using a phase-sensitive lock-in technique is in the form of $\Delta T/T(t)$, namely, the fractional change in transmission, T, which is negative for PA and positive for photobleaching and stimulated emission (SE). The temporal pulse resolution of both laser systems is ~150 fs with pump photon energy, $\hbar\omega$, of either 1.6 eV [below gap (BG), excitation] or frequency doubled to 3.2 eV [above gap (AG), excitation]. The PM data at several wavelengths were normalized between the two laser systems with the fast and slow repetition rates by doubling a suitable frequency in the midinfrared using the OPO system, and measuring the respective $\Delta T/T$ in the visible range.

The steady-state PM spectrum was measured using a standard setup[18] using for excitation an Ar^+ laser beam at $\hbar\omega = 2.5$ eV (AG) or a Ti:sapphire laser beam at 1.55 eV (BG) that were modulated at various frequencies, f; and an incandescent tungsten/halogen lamp that was used as the probe. The PA signal was measured using a lock-in amplifier referenced at f, a monochromator and various combinations of gratings, filters, and solid-state photodetectors to span the spectral range $0.3 < \hbar\omega(\text{probe}) < 2.7$ eV or averaging 6000 scans of pump "on" and "off" using a Fourier-transform infrared (FTIR) spectrometer for $0.05 < \hbar\omega(\text{probe}) < 0.4$ eV. For the PA action spectrum of polarons we used a xenon incandescent lamp of which beam was dispersed through a second monochromator and normalized to obtain the photogeneration response of polarons per incident photon. In order to retrieve the mean lifetime of the photoexcitations, τ, their photoinduced frequency response was measured and fit to an equation of the form $\Delta T(\omega)/T = G\tau/[1+(i\omega\tau)^{\alpha}]$, where G is the generation rate and $\alpha < 1$ is the dispersive parameter that describes the recombination lifetime dispersion of polarons due to disorder in the system. The electroabsorption (EA) spectrum was obtained by measuring the electric-field-induced change in transmission, using a lock-in amplifier set at $2f$ due to field modulation at f; where the film was depos-

ited on a specially designed substrate that contained interdigitated electrodes.[19,20]

The organic diode devices used for measuring the photocurrent consisted of glass substrate coated with indium tin oxide (ITO) and poly(3,4-ethylenedioxythiophene) (PEDOT), which is used for the hole transport layer, and also serves to smooth the contact interface between the active layer and the electrode. The active layer was added by spin coating MEH-PPV/acceptor molecule blend solution over the PEDOT and then capping with 100–150 nm aluminum. Device characterization was performed under illumination by a solar simulator under AM1.5 conditions at an intensity of 100 mW/cm^2.

The MEH-PPV was purchased in powder form from American Dye Source (ADS; Canada) and blended with TNF in toluene solution (AccuStandard), which was drop cast from solution onto a CaF_2, glass, or sapphire substrate to form a film. Although it was claimed[5] that the optimum ratio for CTC formation in MEH-PPV/TNF blend is 1%, we chose to study higher concentrations up to a (1:1) ratio; we also wanted to compare these blends directly to the same weight ratio of MEH-PPV:C_{60}, which is a commonly used blend for photovoltaic devices.

III. RESULTS AND DISCUSSION

A. Absorption and PL spectra

The absorption spectra of MEH-PPV, TNF, and (1:1) MEH-PPV/TNF are shown in Fig. 1(a). For MEH-PPV the band edge is about 2.2 eV, whereas TNF is transparent below 3.0 eV. The absorption spectrum of the MEH-PPV/TNF blend, however extends into the near infrared, and redshifts the first absorption peak of the MEH-PPV constituent. Other *nonadditive* absorption features may arise from increased disorder or altered conjugation lengths of the polymer; however the absorption tail below the gap is not an artifact of crystallization or simply enhanced optical scattering.[6] The relative magnitude and extent of the absorption tail increases with the TNF concentration up to (1:1) ratio. That the absorption tail strengthens as the TNF concentration increases is not surprising since complexing is a quantum-mechanical effect involving wave-function overlap, which accordingly increases with the TNF concentration. The normalized comparison to the solar irradiance at the earth's surface (AM1.5) alludes to its application for solar cells; it is apparent that the extended near-infrared absorption of the MEH-PPV/TNF blend may help generate additional carriers compared to other, more conventional polymer/acceptor blends. Also with absorption extended to the near infrared, we can successfully pump directly below the polymer optical gap when using 1.6 eV photon energy from the various Ti:sapphire laser systems in our arsenal.

We also measured PL quenching and its quantum efficiency (QE) as a function of TNF concentration. As the concentration of TNF increases to 50%, PL intensity drops by at least 3 orders of magnitude (as reported elsewhere[4]) and its QE dropped from 13% in pristine MEH-PPV to ~0.5% in the 50% blend. Similar strong PL quenching has been observed in MEH-PPV/C_{60} composites with increase in photoconductivity by 2 orders of magnitude.[21] This tradeoff has been traditionally explained by ultrafast charge transfer from the polymer to the C_{60} molecules "within 100 fs" of photon absorption in MEH-PPV/C_{60} films.[22,23] In MEH-PPV/TNF blend however, the obtained photocurrent density is in the $\mu A/cm^2$ range, giving rise to a weak photovoltaic effect (see Fig. 2). We note that even though PL quenching is pronounced in the MEH-PPV/TNF blend, it may not necessarily indicate enhancement of mobile charge-carrier density or facilitate photoinduced charge transfer[24] since the underlying mechanism of PL quenching cannot be obtained from cw measurements.

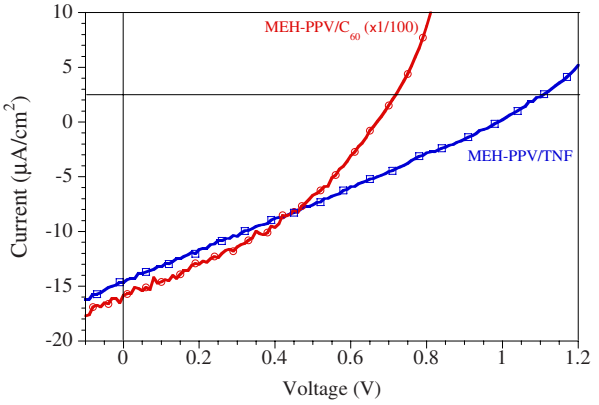

FIG. 2. (Color online) Current-voltage dependence of (1:1) MEH-PPV/TNF (blue squares) and (1:1) MEH-PPV/C_{60} (green circles) in bulk-heterojunction photovoltaic device configuration.

B. Electroabsorption spectroscopy

In order to directly expose the below-gap CTC state in MEH-PPV/TNF blend, we measured the electroabsorption (EA) spectrum in the (1:1) blend. EA has traditionally provided a sensitive tool for studying the band structure of inorganic semiconductors,[25] as well as their organic counterparts.[26–29] Transitions at singularities of the joint density of states respond particularly sensitively to an external field and are therefore lifted from the broad background of the continuous absorption spectrum. The EA sensitivity decreases however, for more confined electronic states, where electric fields of the order of 100 kV/cm are too small of a perturbation to cause sizable changes in the optical spectra. As states become more extended by intermolecular coupling they respond more sensitively to an intermediately strong electric field, F since the potential variation across such states cannot be ignored compared to the separation of energy levels. EA may thus selectively probe extended states and consequently is particularly effective for organic semiconductors, which traditionally are dominated by excitonic absorption. One of the most notable examples of the application of EA spectroscopy to organic semiconductors is polydiacetylene single crystal, in which EA spectroscopy was able to separate absorption bands of quasi-one-dimensional (quasi-1D) excitons from that of the continuum band.[30] The confined excitons were shown to exhibit a quadratic Stark effect, where the EA signal scales with the field squared, F^2,

and the EA spectrum is proportional to the derivative of the absorption respect to the photon energy $[\partial\alpha/\partial\omega(\omega)]$. In contrast, the EA related to the continuum band scales with $F^{1/3}$ and shows Franz-Keldysh-type oscillation in photon energy. The separation of the EA contribution of excitons and continuum band was then used to obtain the exciton binding energy in polydiacetylene, which was found to be ~0.5 eV.[30]

Figure 1(b) shows a prominent broad EA band from 1.2 eV to 1.7 eV that peaks at about 1.4 eV with a shoulder at 1.6 eV; whereas the derivativelike zero crossing at 2.15 eV is due to the Stark shift of the lowest exciton state in the polymer, namely, $1B_u$ exciton.[20] These results clearly show the existence of a CTC state *below the polymer gap*. The strength of the near-infrared feature below the polymer gap indicates that the states involved have a strong dipole moment in agreement with a CT state. We thus conclude that the lowest-energy CTC state is at ~1.3 eV, much lower than that of the CTC state in MEH-PPV/C_{60} blend (measured to be at ~1.5 eV); the difference in the CTC energies may originate from the stronger TNF electron affinity. The depth of the CTC state in MEH-PPV/TNF below the polymer gap raises the question whether a photogenerated CT exciton may be able to readily dissociate under these condition. We will see below that it is indeed much harder to dissociate the CT exciton in MEH-PPV/TNF blend compared to that in MEH-PPV/C_{60} blend, explaining the futility of the former blend for photovoltaic applications.

C. Device current-voltage (*I-V*) characterization

Figure 2 shows the obtained current-voltage relationship of a diode based on (1:1) MEH-PPV/TNF compared to that of MEH-PPV/C_{60}. The power conversion efficiency of the TNF blend device is about 4×10^{-3}%, whereas that of the C_{60} blend device is ~0.4%. The measured current density indicates that the devices made with TNF registers current-density 3 orders of magnitude lower than the typical 10 mA/cm^2 that respectable organic solar cells these days can deliver. The *I-V* crossing at $V=0$ (I_{SC}) has nonzero slope indicating the presence of shunt resistance, which is an additional sign of poor charge mobility in the device. In contrast, the device open-circuit voltage, V_0 is larger in MEH-PPV/TNF blend than that in MEH-PPV/C_{60} in agreement with the larger electron affinity of TNF molecules, which causes a larger LUMO(acceptor) - HOMO(donor) energy difference that is mainly responsible for V_0 [see Fig. 1(b) inset].

D. CW photomodulation spectroscopy

Figure 3 shows the photomodulation spectrum of (1:1) MEH-PPV/TNF blend [Fig. 3(a)] both excited at 2.4 eV, namely above the absorption edge of MEH-PPV but below that of TNF and also BG excitation at 1.55 eV; compared to the PM spectrum of MEH-PPV/C_{60} excited using AG pump [Fig. 3(b)]. The PL has already been subtracted out from the spectrum, so the negative tail evident at higher energy in the TNF blend is not an artifact but photobleaching (PB) from the CTC absorption tail. We also find a strong PA signal

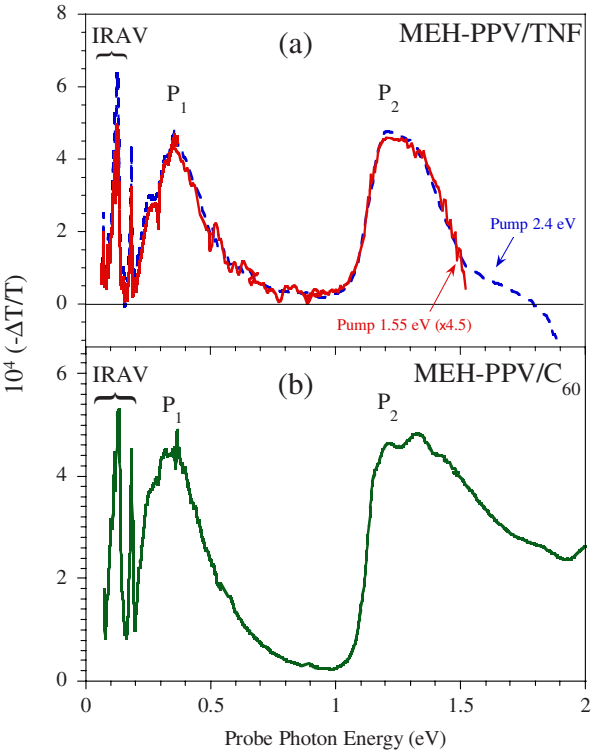

FIG. 3. (Color online) (a) Clockwise photomodulation spectrum of (1:1) MEH-PPV/TNF blend excited at 2.4 eV (blue dotted line), at 1.55 eV (red solid line), compared to (b) the PM spectrum of (1:1) blend of MEH-PPV/C_{60} excited at 2.4 eV. Samples were excited at the same pump intensity of ~70 mW. The polaron bands (P_1 and P_2) and IR-active vibrations (IRAVs) are denoted; the spectra are normalized to the first polaron band, P_1.

when the MEH-PPV/TNF blend is pumped using BG excitation. FTIR spectroscopy PA reveals the existence of various infrared-active vibration (IRAV) modes, ν_1 and ν_2 below 0.2 eV, which have been identified in MEH-PPV/C_{60} blend as due to the modified Raman modes of the polymer chain.[31] The IRAV transitions indicate that P_1 (0.3 eV) and P_2 (1.2 eV) PA bands are associated with charge species and confirm that charges indeed develop along the polymer backbone upon photoexcitation.

The resemblance of the TNF mixture spectrum with that of the C_{60} blend may lead one to expect that their photovoltaic properties would be similar. Alas, photoconductivity is extremely low in the MEH-PPV/TNF blend (Fig. 2). We recognize that if TNF does not cluster sufficiently to form a percolated acceptor network to the anode, the photoinduced charge carriers that escape geminate recombination will become trapped on either the polymer chain or acceptor molecule with little mobility. Such long-lived carriers can accumulate space charge and thus interfere with current transport. Thus, the long-lived polaron signature observed in cw PA does not guarantee mobile charge carriers per se but in this case actually signifies space-charge-limited current, especially when exciting BG.

The PA magnitude is surprisingly large when excited below the gap in the TNF blend. We therefore conclude that the charge photogeneration efficiency is larger for below-gap

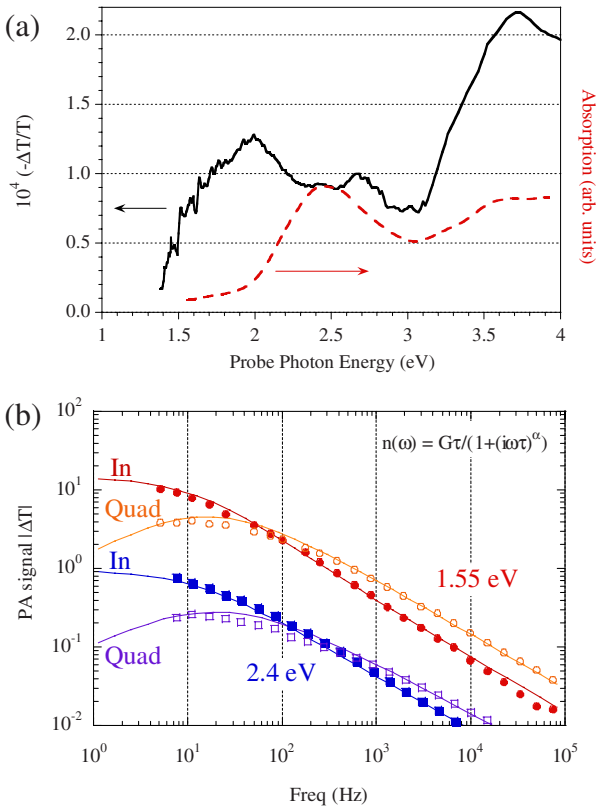

FIG. 4. (Color online) (b) Excitation dependence (action spectrum) of (1:1) mixture of MEH-PPV/TNF per incident photon (black solid line) of P_1 PA band probed at 0.6 eV. The linear absorption spectrum of the blend is also shown for comparison (red dashed line). Data have not been normalized to lifetime (see text). Inset shows lifetime determined by PA frequency-dependence measurement of P_1, comparing photon excitation at 2.4 eV (τ=8 ms) and 1.55 eV (τ=10 ms).

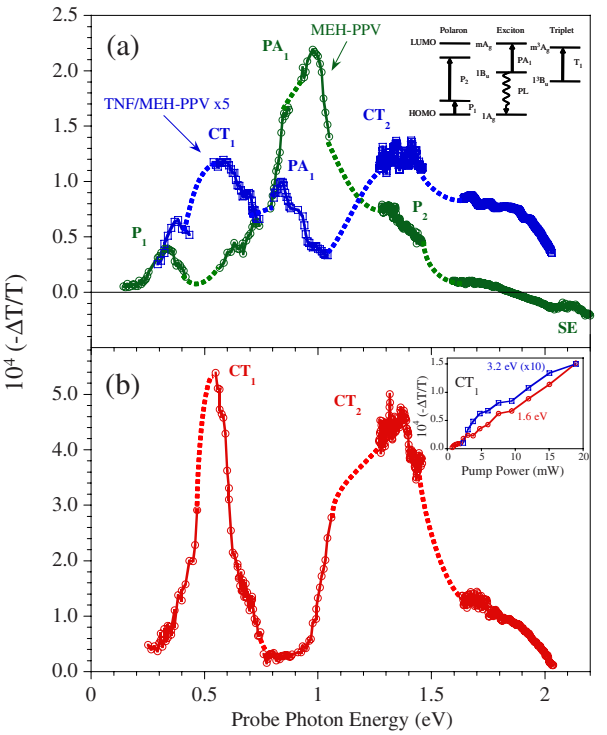

FIG. 5. (Color online) (a) Femtosecond PM spectrum at t=0 of (1:1) MEH-PPV/TNF pumped at 3.2 eV (blue squares) compared to that in pristine MEH-PPV (green circles). The PA bands P_1, P_2, CT_1, and CT_2 are denoted. Inset shows the energy levels and optical transitions of polarons, singlet excitons, and triplet excitons in MEH-PPV. (b) PM spectrum of (1:1) MEH-PPV/TNF blend pumped at 1.6 eV. Inset shows the PA vs pump intensity of (1:1) MEH-PPV/TNF probed at 0.69 eV (CT_1) for both BG and AG excitation

photon absorption. Figure 4(a) shows the excitation dependence (action spectrum) of the polaron P_1 PA band pumped with a Xenon lamp through a monochromator and probed with a Tungsten lamp filtered out above 0.5 eV. The substrate (sapphire) transmission cutoff acts to filter the probe beam below about 0.2 eV; thus only the P_1 band is probed. The strong PA signal per incident photon below the optical gap of the polymer ($\hbar\omega < 2.1$ eV) and far below the absorption edge of TNF is evidence for a large below-gap polaron photogeneration efficiency. It is important to emphasize that excitation dependence generally is not a clear indicator of charge-generation quantum efficiency. Since the PA signal is proportional to both lifetime (and recombination) and generation efficiency, the growth in signal below the polymer optical gap could be attributed to either or both. Indeed, we note that the P_1 lifetime excited below the gap varies as a function of intensity and temperature. However, frequency dependence of P_1 above and below the gap shown in Fig. 4(b) indicates that the polaron lifetime using below-gap ($\tau \sim 10$ ms) and above-gap ($\tau \sim 8$ ms) excitations is similar. Although efficiency cannot be determined absolutely, it is clear that polarons are activated by photon absorption BG, directly into the CTC state below the optical gap of the polymer. The nature of the PA is not very different for 2.1 $< \hbar\omega$(pump) < 3.2 eV where the polymer strongly absorbs light and consequently forms abundant charge carriers. Excitation dependence shows for the MEH-PPV/TNF blend increased polaron generation efficiency below the optical gap *even after lifetime correction*; this is in contrast to MEH-PPV/C_{60} blends.[9] Since the polarons excited BG are generally immobile[9] the enhanced BG photogeneration efficiency indicates that polaron excited AG are also immobile in TNF blends, in contrast to C_{60} blend. The following transient measurements indeed verify this notion.

E. Transient photomodulation spectroscopy

Figure 5(a) shows the transient PM spectra at t=0 in a (1:1) blend of MEH-PPV/TNF compared to pristine MEH-PPV film when pumped at 3.1 eV. The transient PM spectrum of the pristine film contains two PA bands. These are P_1 peaking at ~0.3 eV due to polaron excitations; and PA_1 due to excitons that peaks at ~1 eV.[1] The PA_1 band in the blend is quenched relative to that in the pristine film; PA_1 quenching dynamics are better compared in Figs. 6 and 7. The missing stimulated emission in the composite samples is due to the strongly quenched PL of MEH-PPV in the mixture but may also be due to the ground-state absorption tail in the blend (Fig. 1). The most conspicuous contribution in the ul-

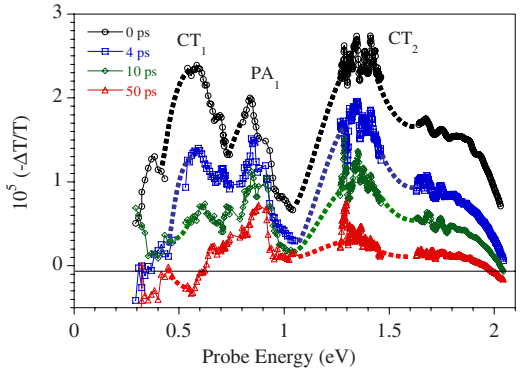

FIG. 6. (Color online) PM spectral dynamics of (1:1) MEH-PPV/TNF blend. The PA bands CT_1 and CT_2 of the CT excitons, and PA_1 of the polymer singlet excitons are denoted.

trafast regime of the blend is the peak around 0.5 eV that appears blueshifted compared to the P_1 peak at ~0.3 eV in cw measurements. The new PA band can be better resolved with BG excitation [Fig. 5(b)], where the PA_1 contribution is completely absent. This is consistent with the interpretation that the PA_1 band is due to excitons, which cannot be photogenerated with BG excitation. Together with the new PA band in the midinfrared spectral range (0.5 eV) we also found a new PA band in the near-infrared spectral range [~1.45 eV; Figs. 5(a) and 5(b)]. Considering the short lifetime of these PA bands (Fig. 7), it would be consistent to consider that the PA bands at 0.5 eV and at 1.45 eV are

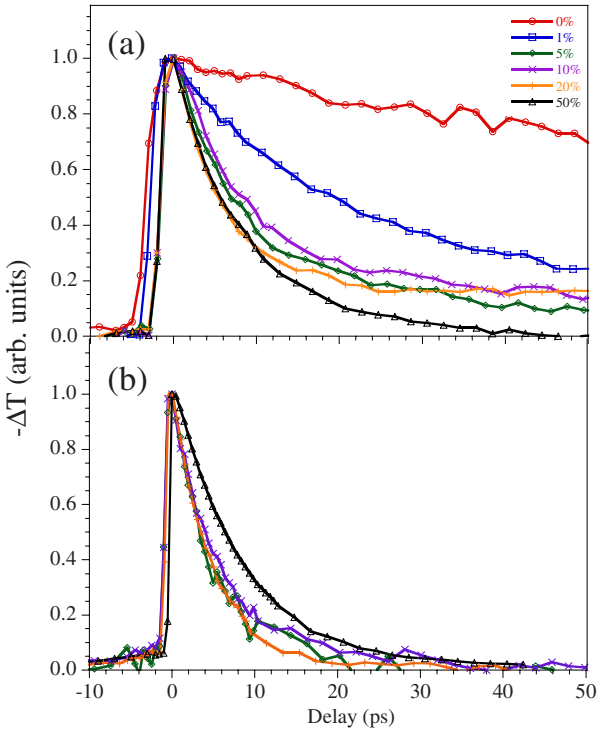

FIG. 7. (Color online) Femtosecond dynamics vs TNF concentration in various MEH-PPV/TNF blends for the CT_1 PA band probed at 0.67 eV and pumped at (a) 3.2 eV (AG) and (b) 1.55 eV (BG). All data have been normalized to their respective peaks at $t=0$.

completely new bands that are associated with the CTC itself; they are therefore labeled CT_1 and CT_2, respectively. In addition to the novel CT bands, the PA_1 exciton band in the blended system is almost completely quenched at $t=0$ when pumped AG of the polymer. Therefore most photogenerated excitons reach the CTC state before the time resolution of the laser system (~150 fs). To ensure that there was no artifact from exciton/exciton annihilation or two photon absorption in our BG experiments, we checked that the transient PA signal is linear versus pump intensity [Fig. 5(b) inset]. Indeed, the pump intensities are well below the threshold for such interactions ($\sim 10^{19}$ cm^{-3}).

Even though most of PA_1 is quenched before the time resolution of our system, its decay at 50% TNF concentration pumped at 3.2 eV (11 ps) is still longer than when pumped at 1.6 eV (8 ps). Spectral dynamics with AG excitation (Fig. 6) show a weak PA_1 remaining at $t>200$ ps. This may explain how the polaron PA is generated in cw PA spectrum even though most of the CT excitations decay within 10 ps, the few reminiscent CT excitons dissociate to form trapped polarons.[17] It was claimed that in a 1% TNF blend, the polaron fingerprint (identical to C_{60} doping) in cw PA forms because a significant amount of (long-lived) photoexcitations escape localized CT back transfer and become trapped.[17] However, at 50% TNF concentration, even though the cw PA spectrum is very similar to that of C_{60} blends, we observe negligible survivability of AG photoexcitations after ~50 ps. Moreover, the same cw PA spectrum arises with BG excitation even though no excitons are photogenerated on the polymer. The conclusion of Ref. 17 cannot explain the same steady-state polaron signature when *all* photoexcitations disappear within $t<50$ ps. Therefore we propose that the long-lived polaron excitations formed with excitation AG and BG in the CTC blend are due to the same process, namely trapping and dissociation of CT excitons in deep traps.

The dynamics of the MEH-PPV/TNF composite reveal (Fig. 7) that all photoexcitations decay within ~10 ps, much faster than the 120 ps exciton lifetime of pristine MEH-PPV. Decay dynamics versus TNF concentration when pumped AG can be further tracked in Fig. 7(a) as normalized dynamic PA signals; concentration dependence of the same blends when pumped BG are reported in Fig. 7(b). PA dynamics are similar in the visible range. Such short lifetimes indicate fast, geminate recombination consistent with the weak cw photocurrent based on the TNF blends (Fig. 2). We note that the CT_1 dynamics show no dependence on modulation frequency, temperature, or magnetic field indicating that its fast dynamics is intrinsic. We thus conclude that the barrier to a back-transfer reaction that is formed in MEH-PPV/C_{60} blends apparently does not form in MEH-PPV/TNF blends. This is a very important ingredient for the minuscule photovoltaic effect for the TNF blends.

We also examined polarization memory decay, $P(t)$, where $P=[\Delta I(\text{par})-\Delta I(\text{per})]/[\Delta I(\text{par})+\Delta I(\text{par})]$ (here $\Delta I(\text{par})$ and $\Delta I(\text{per})$ are the PA with pump/probe polarizations parallel and perpendicular to each other, respectively), at 50% concentration (Fig. 8), and found that it stays constant for the first 20 ps, and then drops to zero by ~50 ps, in contrast to pristine MEH-PPV.[32] Bakulin *et al.*[17] excites at 1.9 eV, above the MEH-PPV:TNF CTC energy and attribute

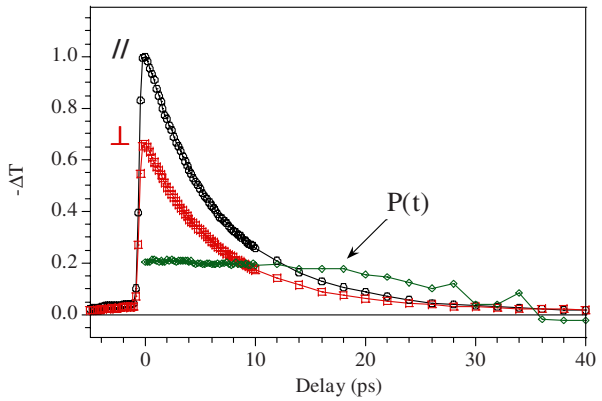

FIG. 8. (Color online) Transient pump/probe polarization in parallel (black circles) and perpendicular (red squares) directions to each other and the obtained transient polarization memory decay, $P(t)$ (green diamonds); see text for P definition.

anisotropy decay at $t<10$ ps to "continuing deformation of the polymer chain that keeps adapting itself to the excess excitation energy." We pump at 1.6 eV, in closer resonance match to the CTC state. Therefore, the photoexcitation stays confined to CTC interaction and thus polarization memory is maintained within ~50 ps. Furthermore, Bakulin *et al.* showed that at 1% TNF concentration, anisotropy *increases* after 50 ps, interpreted as fast decay of short-lived subensemble and the residual domination of the long-lived subensemble anisotropy. These long-lived subensembles are absent in our 50% TNF concentration, either because the short-lived species are dominant at higher TNF concentration or, at lower photon energy, we only excite the short-lived species.

We have described in this paper the transient PA spectrum of the pristine polymer in a 1D "conventional" context, assigning transitions to intrachain exciton and polaron states. A recent theoretical work discusses the formation of photoinduced charge-transfer excitons as a superposition of neutral exciton and charge-ion species.[33] The authors calculate PA spectra based on high-order configuration interactions in the excited states for two coupled phenylenevinylene (PPV) short chains revealing distinct CT exciton and polaronlike PA signatures in the MIR spectral range, which are nearly *indistinguishable* from those of the more traditional, 1D exciton, and polaron models.[34] According to their theory, AG excitation generates predominately the optical pure exciton along with a small population of CT excitons, which evolve to predominately lower-energy CT excitons. One can imagine by extension that direct BG resonant excitation into the CTC would produce a large population of CT excitons that would eventually release a high yield of lower-energy polaron pairs and manifest their accompanying IRAVs. In this case, the CTC may have a charged component such that the steady-state polaron is not a different species but a branch from the mixed state origin. Since polaron pairs are not affected by interchain charge transfer, their transitions occur at roughly the same energy as in 1D models. The CTC is very different when the two neighboring organic molecules are not the same, such as in MEH-PPV/TNF.[34] In this case the CT transitions are substantially blueshifted with respect to the polaron transitions. This model actually is in very good agreement with what we found here when excited below the gap, directly into the CTC state. Furthermore, the obtained long-lived and predominately parallel polarization memory of CT_1 indicates that is strongly aligned along the CTC photoexcitation (pump) dipole, viz., both CTC and CT_1 lie perpendicular to the polymer chain. Such evidence naturally extends the merits of the model presented in Ref. 34 for the excited processes of acceptor/donor blends. Polarization memory decay with AG and BG excitation are underway to finally elucidate the character of the primary photoexcitation species in these materials.

IV. CONCLUSIONS

In this paper we used a variety of transient and cw probes to study the primary and long-lived photoexcitations in MEH-PPV/TNF blends. We found that the photophysics in these blends is dominated by a CTC state below the polymer gap. We directly revealed the below-gap CTC state using electroabsorption spectroscopy; the lowest CTC is at ~1.3 eV, deep in the gap of the polymer chains. By directly exciting the CTC at 1.6 eV, we recover a cw PM spectrum with the same spectral features as the same blend, and a comparable MEH-PPV:C_{60} blend excited at 2.4 eV, above the polymer optical gap. This indicates that charge carriers are photogenerated in all cases, when photoexcited both above and below the gap. However, photoconductivity in a diode based on MEH-PPV/TNF blend is extremely low because the photogenerated CT excitons do not survive long enough to efficiently dissociate and avoid geminate recombination and/or TNF does not cluster to form a percolated network to the electrodes as C_{60} does. We also report ultrafast transient-photomodulation measurements of the CT excitons of a 1:1 MEH-PPV/TNF blend in a broad spectral range from 0.2 to 2.0 eV with 150 fs time resolution. Dynamic time sweeps reveal that the CT excitons recombine within 8–10 ps with strongly (but not completely) quenched exciton yield when pumped above the gap.

We conclude that the pathway to long-lived charge generation is the same for both above- and below-gap excitations, and involves the CTC state. Considering the charge photogeneration mechanism, perhaps the excess energy is dissipated in a heat bath reservoir, which eventually increases the local temperature of the sample. If there exist interface barriers between MEH-PPV and TNF, then the increase in the bath temperature might thermally generate separated charges on the HOMO of the polymer and LUMO of the TNF molecule, similarly as in PIN junction formed with inorganic semiconductors.[35] We conclude that in this paper the inefficiency of the MEH-PPV/TNF blend for photovoltaic applications was exposed by the fast dynamics obtained for the CT photoexcitations.

*Author to whom correspondence should be addressed; val@physics.utah.edu

[1] C.-X. Sheng, M. Tong, S. Singh, and Z. V. Vardeny, Phys. Rev. B **75**, 085206 (2007).
[2] C. Winder and N. Sariciftci, J. Mater. Chem. **14**, 1077 (2004).
[3] N. H. Karam, R. R. King, M. Haddad, J. H. Ermer, H. Yoon, H. L. Cotal, R. Sudharsanam, J. W. Eldredge, K. Edmondson, D. E. Joslin, D. D. Krut, M. Takahashi, W. Nishikawa, M. Gillanders, J. Granata, P. Hebert, B. T. Cavicchi, and D. R. Lillington, Sol. Energy Mater. Sol. Cells **66**, 453 (2001).
[4] J. Y. Kim, K. Lee, N. E. Coates, D. Moses, T.-Q. Nguyen, M. Dante, and A. J. Heeger, Science **317**, 222 (2007).
[5] A. A. Bakulin, S. G. Elizarov, A. N. Khodarev, D. S. Martyanov, I. V. Golovnin, D. Y. Paraschuk, M. M. Triebel, I. V. Tolstov, E. L. Frankevich, S. A. Arnautov, and E. M. Nechvolodova, Synth. Met. **147**, 221 (2004).
[6] D. Y. Paraschuk, S. G. Elizarov, A. N. Khodarev, A. N. Shchegolikhin, E. M. Nechvolodova, and S. A. Arnautov, JETP Lett. **81**, 467 (2005).
[7] V. V. Bruevich, T. S. Makhmutov, S. G. Elizarov, E. M. Nechvolodova, and D. Yu. Paraschuk, J. Chem. Phys. **127**, 104905 (2007).
[8] J. J. Benson-Smith, L. Goris, K. Vandewal, K. Haenen, J. V. Manca, D. Vanderzande, D. D. C. Bradley, and J. Nelson, Adv. Funct. Mater. **17**, 451 (2007).
[9] T. Drori, C.-X. Sheng, A. Ndobe, S. Singh, J. Holt, and Z. V. Vardeny, Phys. Rev. Lett. **101**, 037401 (2008).
[10] P. Panda, D. Veldman, J. Sweelssen, J. J. A. M. Bastiaansen, B. M. W. Langeveld-Voss, and S. C. J. Meskers, J. Phys. Chem. B **111**, 5076 (2007).
[11] G. Ruani, C. Fontanini, M. Murgia, and C. Taliani, J. Chem. Phys. **116**, 1713 (2002).
[12] M. Hallermann, S. Haneder, and E. Da Como, Appl. Phys. Lett. **93**, 053307 (2008).
[13] C. Im, J. M. Lupton, P. Schouwink, S. Heun, H. Becker, and H. Bässler, J. Chem. Phys. **117**, 1395 (2002).
[14] J. E. Kuder, J. M. Pochan, S. R. Turner, and D. F. Hinman, J. Electrochem. Soc. **125**, 1750 (1978).
[15] J. G. Müller, J. M. Lupton, J. Feldmann, U. Lemmer, M. C. Scharber, N. S. Sariciftci, C. J. Brabec, and U. Scherf, Phys. Rev. B **72**, 195208 (2005).
[16] W. D. Gill, J. Appl. Phys. **43**, 5033 (1972).
[17] A. A. Bakulin, D. S. Martyanov, D. Y. Paraschuk, M. S. Pshenichnikov, and P. H. M. van Loosdrecht, J. Phys. Chem. B **112**, 13730 (2008).
[18] T. Drori, E. Gershman, C.-X. Sheng, Y. Eichen, Z. V. Vardeny, and E. Ehrenfreund, Phys. Rev. B **76**, 033203 (2007).
[19] S. Jaglinski, Ph.D. thesis, University of Utah, 1996.
[20] M. Tong, C.-X. Sheng, and Z. V. Vardeny, Phys. Rev. B **75**, 125207 (2007).
[21] X. Wei, Z. V. Vardeny, N. S. Sariciftci, and A. J. Heeger, Phys. Rev. B **53**, 2187 (1996).
[22] D. Moses, A. Dogariu, and A. J. Heeger, Phys. Rev. B **61**, 9373 (2000).
[23] P. B. Miranda, D. Moses, and A. J. Heeger, Phys. Rev. B **64**, 081201(R) (2001).
[24] S. Cook, H. Ohkita, J. R. Durrant, Y. Kim, J. J. Benson-Smith, J. Nelson, and D. D. C. Bradley, Appl. Phys. Lett. **89**, 101128 (2006).
[25] R. K. Willardson and A. C. Beer eds., *Semiconductors and Semimetal* (Academic, New York, 1972), Vol. 9.
[26] L. Sebastian, G. Weiser, and H. Bässler, Chem. Phys. **61**, 125 (1981).
[27] G. Weiser, Phys. Rev. B **45**, 14076 (1992).
[28] D. Guo, S. Mazumdar, S. N. Dixit, F. Kajzar, F. Jarka, Y. Kawabe, and N. Peyghambarian, Phys. Rev. B **48**, 1433 (1993).
[29] M. Liess, S. Jeglinski, Z. V. Vardeny, M. Ozaki, K. Yoshino, Y. Ding, and T. Barton, Phys. Rev. B **56**, 15712 (1997) and references therein.
[30] L. Sebastian and G. Weiser, Phys. Rev. Lett. **46**, 1156 (1981).
[31] C.-X. Sheng, Ph.D. thesis, University of Utah, 2005.
[32] S. Singh, T. Drori, and Z. V. Vardeny, Phys. Rev. B **77**, 195304 (2008).
[33] Z. Wang, S. Mazumdar, and A. Shukla, Phys. Rev. B **78**, 235109 (2008).
[34] D. Psiachos and S. Mazumdar, arXiv:0901.3121 (unpublished).
[35] W. J. Potscavage, Jr., S. Yoo, and B. Kippelen, Appl. Phys. Lett. **93**, 193308 (2008).
[36] S.-H. Jin, M.-S. Jang, H.-S. Suh, H.-N. Cho, J.-H. Lee, and Y.-S. Gal, Chem. Mater. **14**, 643 (2002).
[37] Y. Yamamoto, T. Fukushima, Y. Suna, N. Ishii, A. Saeki, S. Seki, S. Tagawa, M. Taniguchi, T. Kawai, and T. Aida, Science **314**, 1761 (2006).